UNIVERSITY OF PUERTO RICO AT MAYAGÜEZ

MAYAGÜEZ, PUERTO RICO

DEPARTMENT OF ELECTRICAL AND COMPUTER ENGINEERING

WaveSphere: Final Report

A REPORT SUBMITTED AS A PARTIAL REQUIREMENT OF THE MICROPROCESSOR INTERFACING COURSE ICOM-5217

by

Adrián Ildefonso - Project Leader
Daniel Santiago
Nelián Colón
Samuel Rodríguez

For: Dr. M. Jiménez
Course: ICOM 5217, Section 088
Date: May 10, 2013

Abstract

Wave post-breaking dynamics is a phenomenon that is not yet well understood. This work presents the design process and a discussion of the operation of a device to measure variables that are essential to the physics of wave breaking. The aforementioned device is a spherical drifter with a diameter of 7.5cm designed to closely imitate the dynamics of a particle in the water. It is equipped with 3-axis accelerometer, gyroscope and magnetometer, allowing the drifter to measure its motion to nine degrees of freedom. This will allow the researchers to reconstruct the device trajectory in the wave via dead reckoning. A GPS module, on-board flash memory for data storage and a wireless communication module for data retrieval are also integrated. An MSP430FR5969 from Texas Instruments controls and establishes communication between system components. The designed user interface allows the researchers to interact with the drifters wirelessly as well as retrieve the data that has been captured after an experiment. It is expected that, when used in synergy, multiple units will be able to greatly help researchers understand the dynamics of wave breaking.

Table of Contents

List of Figures

List of Tables

1. Introduction

Although waves are abundant at sea and everyone who has been near a shoreline has seen and interacted with a wave, most people do not think about the wave-breaking phenomena when enjoying their time in the water. However, this topic is very important for the researchers at the Fluid Mechanics and Ocean Engineering Laboratories at the University of Puerto Rico at Mayagüez, which are directed by Dr. Miguel Canals. The natural physics and motion dynamics of the wave-breaking phenomena have not been thoroughly studied because of the difficulty encountered when trying to measure the characteristics of the waves.

A novel way to study these dynamics is by developing an instrument, also referred to from hereon as drifter, that will ride with the waves and take measurements during the wave-breaking process. This is the approach that the researches have taken as part of the NSF Funded project titled "Lagrangian Observations of Turbulence in Breaking Waves". Currently, the researchers[1] working on this project have an assembled prototype with which they have been performing experiments. This drifter consists of a small spherical plastic casing which houses a series of sensors, a microSD card, a microcontroller and power management components.

However, their prototype has a series of issues that need to be addressed so that the overall functionality is improved. One example of a current issue is that design being used has an external button to activate the sphere. The way in which the button was mounted on the plastic spherical casing allowed for the water to leak inside the casing, damaging the electronic components. Another issue with the current design is the lack of location information. Once the drifter has been deployed and the experiment has concluded, the researchers must retrieve the drifter. However, they have lost drifters because the waves have taken them away, making them impossible to find.

The objective of this project is to improve the overall design of the drifter currently being used by the researchers by addressing the previously mentioned issues, as well as other issues not mentioned. Because the drifters will have more capabilities, a base station must also be designed so as to allow for easy management of the individual drifters through a custom application displayed to the user via a graphical interface.

This work presents the design process of a spherical drifter that will aid the researchers in taking the aforementioned measurements. A system overview is presented so as to give the reader a better idea of the solution proposed by this work. This is followed by a thorough discussion of the hardware and software design process. Figures, tables and calculations are presented along the way to support the claims made by this work and aid the reader in understanding certain aspects of the design process. Finally, a brief recommendation of work that could be done in the future to improve the current prototype is given.

[1] From hereon, the word researchers and users will be used interchangeably.

2. Theoretical Background

Wave breaking is a complex phenomenon that has been thoroughly studied in the field of oceanography and fluid mechanics[2]. However, there are few studies that focus on the turbulence formed on the surf zone, a phenomenon that is difficult to replicate in a laboratory. The research project titled "Lagrangian observations of turbulence in breaking surface waves" aims at studying this phenomenon. Some of the reasons to research this area include understanding the intensity of energy dissipated, the mechanics behind sediment transport, erosion, the diffusion of organisms and contaminants in the surf zone, among many others [2]. Being a fundamental problem for fluid mechanics, the observations and results from this projects might have more applications than those currently envisioned by the researchers.

In fluid mechanics, there are two ways to describe flow: Eulerian and Lagrangian. The Eulerian approach describes what is happening at a given location for a given time, whereas the Lagrangian approach describes the history of the particle exactly [3]. Looking at these two terms from a sensors point of view, an Eulerian sensor would be at a fixed position recording data over time, whereas a Lagrangian sensor would move with the particles of the fluid while recording data. It is easy to see that for the study of wave breaking phenomena a Lagrangian sensor would be preferable, as the path of the waves are unpredictable and an initial location cannot be determined before the event occurs.

Because they are intended to measure important variables in the wave breaking process, the Lagrangian sensor must have a geometry different than traditional drifters. For this particular application, a spherical drifter is needed, so that it can flow with the water just as a sediment particle would. It was determined in [4] that the sphere diameter to wave height ratio should be minimized, which is why a spherical 7.5 cm diameter capsule was assembled, a size that permits the necessary components to reside within a plastic casing. The drifters are to be released within breaking waves to measure essential variables that are related to the wave breaking process in an interest to revolutionize the way this phenomenon is studied [4]. These variables include acceleration, rotation and orientation data.

By taking measurements of the drifter's acceleration, rotation and orientation, the researchers hope to recreate the drifters trajectory via dead reckoning. Dead reckoning consists of calculating the displacement from a previous known position by using the integral of measured velocity and information on the direction in which the object is headed [5], which can be determined by the rotation and orientation information. The velocity can be found by integrating the measurements of acceleration already taken. Doing this for all the data points gathered while the drifter is in motion will yield the position of the drifter across time, from which the trajectory can be reconstructed. Since the drifters follow the flow of water, the trajectory of the drifters will give them the trajectory taken by the flow of water. This will allow them to visualize the currents and vortices formed after a wave breaks.

[2]This section is based on the authors' interpretation of the unpublished thesis of Andre Amador, one of the researchers working on the project titled "Lagrangian observations of turbulence in breaking surface waves".

The data required to recreate the trajectory of the drifters via dead reckoning can be captured by an accelerometer, a gyroscope and a magnetometer. Together, these three sensors are also known as a nine degree-of-freedom inertial measurement unit. These three sensors, together with the microcontroller (MCU), are the main components of the drifters presented in this work. The design and implementation was done around the sensors, as these were selected first in order to make sure that they met the researcher's requirements.

3. System Overview

The proposed system consists of two parts, a spherical drifter which will be deployed right into the waves and a base station that will be used to control the drifters. The researchers that will use the drifters to conduct their experiments will use a personal watercraft (PWC) to deploy the drifters at the point where the wave breaks and retrieve them after the experiment has concluded. Figure 1 shows the scenario of a single experiment. The base station will reside in the PWC and the researchers will throw the drifters into an emerging wave so that when it breaks the drifter is already recording data from the sensors.

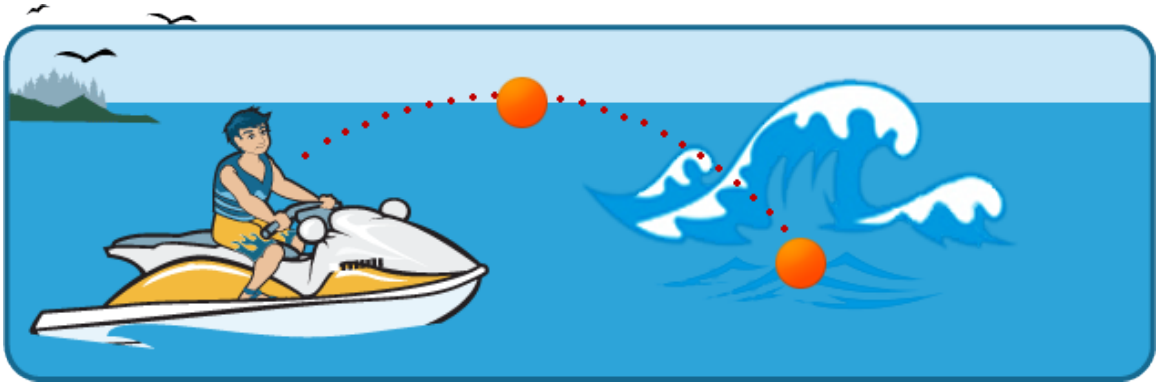

Figure 1: A graphical depiction of the deployment process of the drifters. Image adapted from [1].

3.1 Drifters

The drifters consist of a plastic sphere of about 7.5cm in diameter inside which all the electronic components reside. The plastic sphere can be opened and closed: the two halves of the sphere are threaded at the rim near the diameter so that they can be screwed in together. The drifters are equipped with various sensors, GPS and wireless modules, among other components. A detailed explanation of the components that make up the drifters follows.

Sensors

The drifters are equipped with an accelerometer to measure the changes in acceleration

of the device, a gyroscope to measure the changes in orientation and a magnetometer to measure the orientation with respect to the Earth's magnetic north. All three sensors take data from three axes. Together, they make up what is known as a nine degree-of-freedom inertial measurement unit. As previously mentioned, the data collected from these three sensors is used to determine the path that the drifter has taken within the wave.

GPS and XBee Modules

After an experiment has concluded, the users must manually retrieve the drifters from the water. To aid in this process, the drifters are equipped with a GPS and an XBee module. After all the necessary data has been collected, a process which takes about 30 seconds, the drifter acquires its current location and sends it to the base station through the Xbee module. This allows the users to easily locate and retrieve the devices.

The Xbee Module also serves to receive commands from the base station in order to change between operating modes. The different operating modes of the sphere can be found in Section 9. It can also be used to wirelessly retrieve the acquired data from the drifter to the base station.

Battery Powered

Because of the necessity for portability, the drifters are battery powered. Each device is equipped with a Lithium-Ion 3.7V rechargeable battery. There is also a micro-USB port that can be used to recharge a depleted battery. In order to make the drifter air-tight so that no water can enter the spherical plastic case, the port used to recharge the battery resides inside the sphere, which is why it must be twisted open in order to access the port.

RF Wakeup Module

Since the plastic sphere has to be air-tight, adding a physical button or some other type of mechanism on the outside of the sphere in order to activate the drifters proved to be unfeasible as this could potentially create leaks which would damage the electronic components inside. In order to solve this problem, the drifter is equipped with an RF receiver and antenna that responds to 125kHz signals, the same ones found in RFID card readers. The purpose of this module is to wake up the system and activate the drifter once the 125kHz signal has been applied. It replaces an external button or other external actuation mechanism.

SD Card and Mass Storage

Data acquired is stored in a microSD card embedded in the drifters. There are three ways to retrieve the data from the drifters: wirelessly through the XBee module, by removing the SD card and inserting it into a card reader connected to a computer or through the on board micro-USB port. The drifters are equipped with a module that allows them to behave like a mass storage device when connected to a computer. Thus the users can browse the files just as they would when browsing through the files in a thumb drive.

Indicator LEDs

There are four LED indicators that serve as the user interface. Each one has a different function as follows:

Red LED When the red LED is on, it means that the system is powered on. If it starts flashing, it means that the battery level is low.

Blue LED When the drifter is connected through the micro-USB port, the blue LED turns on when the battery is charging. Once the battery is fully charged, the LED turns off.

Green LED The green LED is powered on when the XBee ZB module is turned on and ready to transmit or receive data.

Amber LED The amber LED is powered on when the GPS module has acquired a fix, or when it is able to acquire satellite signals to determine its position.

3.2 Base Station

The base station consists of an RFID reader, an XBee module and a computer on which a custom application with a graphical user interface (GUI) resides. The GUI can manage and communicate with several drifters at the same time. The RFID reader and XBee ZB are powered through a USB port on the computer. A brief explanation of each of these components and their role on the system follows.

RFID Reader

The RFID Reader is used to generate a 125kHz signal that is received by the RF Wakeup module inside the drifter. Once the drifter comes within a certain proximity of the RFID reader, it will be activated by the wakeup module.

XBee Module

The XBee module on the base station is the counterpart of that found inside the drifter: it completes the communication path between the drifters and the host computer. Through this module, the host computer is able to send commands to the drifters as well as receive the experimental data sent by the drifters to the base station. The module then passes the data to the host computer, completing the data transmission transaction.

Graphical User Interface

The researcher's current experimental setup allows them to have a computer on board the PWC without risking water damage. The computer on the PWC is loaded with a custom application that consists of a Graphical User Interface (GUI). This application allows the users to communicate with the drifters in a simple manner. Through a series of windows and buttons the user can intuitively navigate through the application in order to perform tasks such as changing the operating modes of the spheres.

The full capabilities of the GUI along with instructions on how to navigate through it and perform the various tasks for which it was developed can be found in the User's Guide which located in Appendix A.

4. Block Diagram

Figure 2 shows the block diagram for each of the drifters while Figure 3 shows the block diagram for the base station. Both diagrams contain the model numbers of the components and, in the case of the drifter block diagram, the types of connections required to the microcontroller unit (MCU) and the amount of lines needed for each connection. A list of the components in each block diagram along with a brief explanation for each one follows.

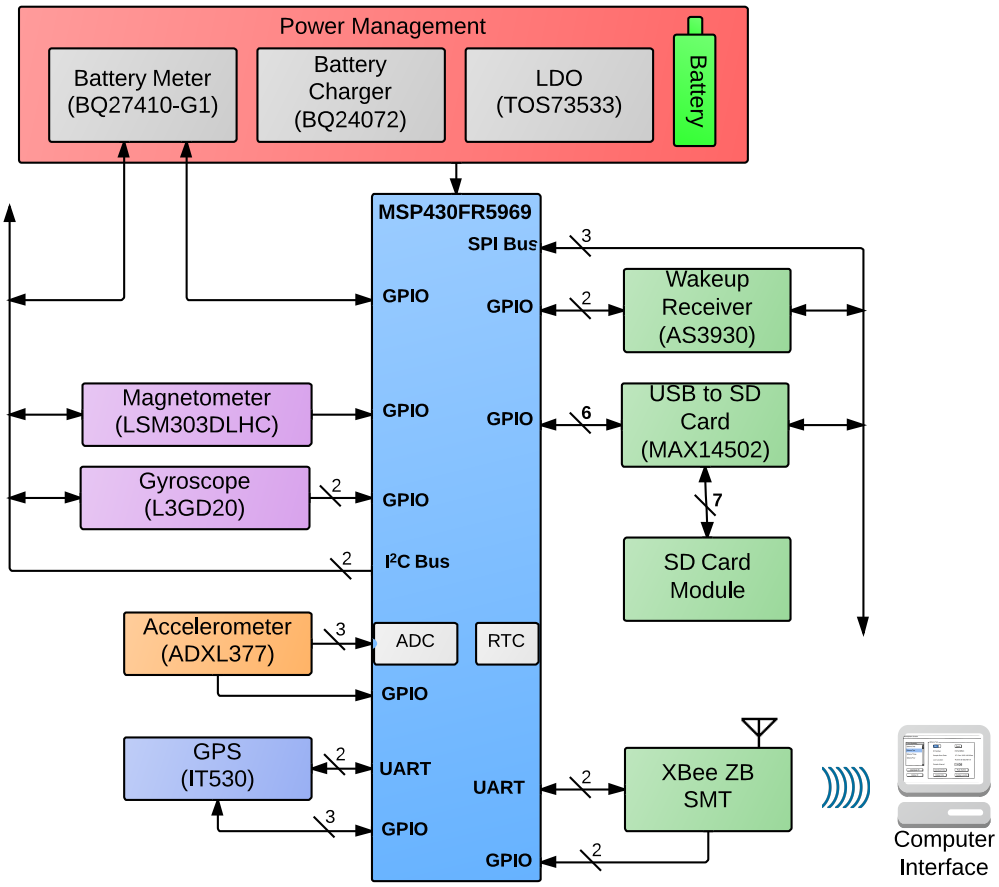

Figure 2: Block Diagram for the Drifter

4.1 Drifter Block Diagram

1. **Microcontroller** - Needed in order to be able to control and establish the communication between components as well as process the output of the sensors.
2. **Battery** - Required to provide the necessary power to the drifters because the electrical components are enclosed by a sphere.
3. **Power Management Circuit** - Composed of an LDO, a battery charger and a battery meter. It is used to regulate the power provided by the battery, re-charge the battery

once it has been depleted and to measure the amount of charge left on the battery.

4. **GPS Module** - Needed in order to know the precise location of the drifters when the user has to recover them after they have been thrown at sea for an experiment.
5. **Gyroscope** - Used to determine the rate of change of the orientation of the drifter while being carried by a wave.
6. **Accelerometer** - Used to measure the acceleration of the drifter while being carried by the waves.
7. **Magnetometer** - Used to determine the orientation of the drifter with respect to the Earth's magnetic north while it is being carried by a wave.
8. **Analog to Digital Converter (ADC)** - Needed in order to take the data from the accelerometer, which has an analog output, and convert it to digital signals so that the MCU can read them. It is integrated within the MCU.
9. **SD Card and SD to USB Converter** - The SD Card is used to save the data captured by the sensors during an experiment. The SD to USB converter will be used to allow the drifter to function as a mass storage device when connected to a Host computer via USB.
10. **XBee ZB Module** - Used to connect the spheres with a central base so that data can be retrieved without having to open the spheres.
11. **RF Wakeup Module** - Used to wirelessly wake up the drifter from low power mode via an RF signal.

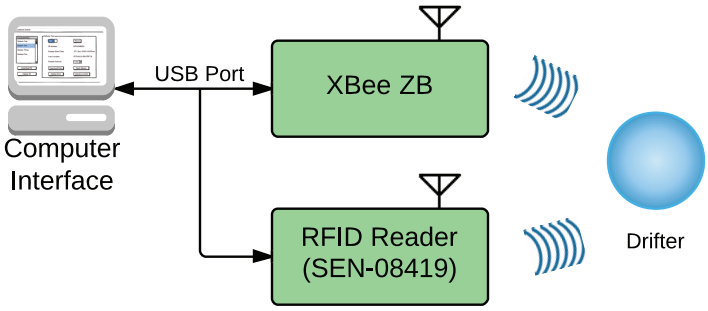

Figure 3: Block Diagram for the Base Station

4.2 Base Station Block Diagram

1. **XBee ZB Module** - Used to communicate with the drifters in order to send commands to switch operating modes and retrieve collected data.
2. **RFID Reader** - Used to generate the 125kHz signal required by the RF Wakeup module in the drifters to wake them up from low power mode.
3. **Computer** - Used to run a custom application that will be used to send commands and data to the drifters through the XBee. A USB port in the computer will power the other devices in the base station.
4. **Power Management Circuit** - Composed of an LDO, a battery charger and a battery meter. It is used to regulate the power provided by the battery, re-charge the battery

once it has been depleted and to measure the amount of charge left on the battery.

5. Power Analysis

The power analysis consists of four main parts: logic compatibility, driving capability, power supply design and battery life estimate. The purpose of this analysis is to ensure that power requirements for each component are satisfied in order to guarantee their proper functionality. A supporting thermal analysis is performed on selected ICs.

5.1 Logic Compatibility

Table 1 shows all the digital components in the system along with their input and output digital voltage levels. Only two digital components communicate with each other: the SD Card to USB converter IC and the SD Card itself. It is easy to see from Table 1 that the logic voltage levels between these two devices are compatible. In addition to this, all components communicate with the MCU. It can also be seen that all the devices are logically compatible with the MCU except for the battery gauge, which communicates with the MCU through an I^2C interface and has a V_{DD} of 2.5V. In order to make them compatible, a bi-directional logic level shifter from Texas Instruments was used and can be found in the schematic. It can be seen in the table that by using the aforementioned level shifter, communication between the battery gauge and the MCU is now possible.

Table 1: Component Logic Levels and I/O Currents

Component	V_{DD}	V_{IH}	V_{IL}	V_{OH}	V_{OL}	I_{OUT}	I_{IN}	I_{LEAK}
MSP430FR5969[3]	3.3	2.1	0.75	3.2	0.2	45 mA[4]	50 nA	50 nA
Magnetometer[5]	3.3	2.64	0.66	3.3	0	3 mA	10 μA	10 μA
XBee	3.3	2.64	0.66	2.706	0.594	4 mA	0.5 μA	0.5 μA
RF Wakeup	3.3	1.914	0.99	2.9	0.4	21 mA	100 nA	100 nA
Gyroscope	3.3	2.64	0.66	2.64	0.66	100 μA	10 μA	10 μA
GPS	3.3	2	0.8	2.4	0.4	8 mA	10 μA	10 μA
Battery Gauge[6]	2.5	1.2	0.6	2	0.4	3 mA	10 μA	0.3 μA
SD Card[7]	3.3	2.06	0.83	2.48	0.41	100 μA	10 μA	10 μA
Power Switch	3.3	2.2	1.1	3.3	0	10 mA	0 mA	0.3 μA
SD Card to USB Converter	3.3	2.06	0.83	2.48	0.41	100 μA	2 μA	1 μA
Level Shifter[8]	2.5	1.7	0.7	2.5	0	100 μA	20 μA	10 μA

5.2 Driving Capability

In order to ensure that no component draws more current than the one its driver can provide, a weakest driver analysis should be performed. Table 1 shows a list of the available currents found in the data sheets and other sources. The components and their connections are shown in the block diagram depicted in Figure 2.

Since I^2C is a standard, there would be no problems if the level shifter was not present. However, since this component is the weakest driver, the analysis must be performed. The output current of this component is 100 μA in order to maintain the voltage levels specified in Table 1. It can be seen that this current is greater than the sum of input currents of the components connected to the bus: 10 μA for the Gyroscope, 10 μA for the Magnetometer and 50 nA for the MCU.

Since the components connected through UART and Software UART are point to point connections and since the MCU has such a low input and leakage current, the Xbee and GPS modules do not have a problem driving the MCU. Finally, for the SPI Bus, the weakest driver is the SD Card to USB Converter with an output current of 2 μA. It can be seen from Table 1, that this current is greater than the sum of input currents for the other components: 100 nA for the RF wakeup and 50nA for the MCU.

With this analysis, one can conclude that all ICs can drive their respective loads.

5.3 Power Supply Design

In order to design the power supply that is used by the system, the worst case quiescent current of each component was taken into account. Although not all components operate at the same time, it is ensured that the system will continue to function properly for the worst possible case by performing the analysis in this manner. To ensure proper operation of the system, the Low-Dropout Regulator (LDO) must supply enough current for the entire system. Table 2 shows a list of components along with the worst case quiescent current of each of them. By adding all the current, a maximum current consumption of 181 mA was determined. The LDO is rated for a maximum output of 500 mA, which is well above the determined usage. In order to complete the power supply circuit, a USB Battery Charger and a Battery Meter were added as well. Note that since the level shifters are powered by the 2.5V regulated output of the Battery Meter, they have not been included in these calculations.

Table 2: Worst Case Quiescent Currents for components

Component	$I_{DD(Active)}$ (μA)
MSP430FR5969	1600
3-Axis Accelerometer	300

Component	$I_{DD(Active)}$ (μA)
Magnetometer	110
XBee	45000
RF Wakeup	2.7
Gyroscope	6100
GPS	26140
SD Card	100000
Power switch	1
SD to USB	37
LDO	65
Battery Charger	1500
Battery Meter	103
Total	180958.7

5.4 Thermal Analysis

A thorough thermal analysis was performed on the MCU and all the power management ICs to determine whether they would exceed the thermal limits of their package under regular operation in our system. The expected operating junction temperature was calculated using the junction-to-ambient thermal resistance and the power dissipated by each IC. It was determined that no additional heat dissipation technique as needed to guarantee the proper operation of the ICs since all the calculated junction temperatures were well below the maximum operating junction temperature specified in the manufacturer's datasheets. The thorough and detailed analysis can be found in Appendix D.

6. Timing Analysis

The timing analysis consists of three main parts: Time bases, Point-to-point communication, and analog considerations. The purpose of this analysis is to ensure that no signal is transmitted at a faster frequency than the one its receiver can read, thus guaranteeing communications functionality and interoperability between all components and the MCU.

6.1 Time bases

This section compares the maximum external clock frequencies of all components and their communication ports to make sure that no component is overclocked by the MCU and that all synchronous communication can be performed at the speed of the MCU's clock. Table 3 shows the frequency specifications for the components. Since the sample frequency is a relatively low 250Hz, there is complete compatibility between the MCU and all components. The MCU can run at a clock frequency of up to 16MHz. For I^2C

communications, the fast mode standard of 100-400kHz is being used, since all components are compatible with it. For SPI communications, the signaling rate can be changed between devices. For the slowest device, the RF wakeup, a rate of 1MHz is being used. For the SD card, a rate of 4MHz was implemented. Two components are communicating with the MCU through UART, the XBee wireless receiver/transmitter and the GPS receiver. Both of them communicate with a baud rate of 9600. Since they must be used at the same time, two separate UART buses were used, and since the MCU did not have enough UART state machines, Software UART through GPIO ports was implemented for the GPS receiver.

Timers Three timers are needed in total, two for sampling and one for implementing UART via software. The first sampling timer controls the sample frequency for all the components. In order to sample at an accurate frequency of 250Hz, an external crystal with a frequency of 12MHz is being used. To achieve this, the crystal feeds the master clock and sub-main clock (MCLK and SMCLK, respectively), and the terminal count is set to 48,000 with a prescale divider of one. The second sampling timer is used to count the time and update the timestamp whenever a sample is taken. The prescaler of this timer is set to one and the terminal count is set to 12,000. Thus, this timer is ticking at 1kHz, and each count of the timer corresponds to 0.1ms of elapsed time. This is more than enough precision for the intended application. An additional timer is needed for the software UART implementation, which uses the capture/latch feature of the timer to detect incoming data packets and interrupt the MCU. It also uses the interrupt feature for the transmitting function. After a bit is transmitted through the UART bus, the timer is set up to fire at the time in the future when the next bit must be output on the bus.

12MHz Crystal Oscillator The reason why a 12MHz crystal was chosen is because the USB-to-SD card reader needs a 12MHz clock input from the MCU for establishing USB communications. Additionally, the GPS and Xbee modules communicate through UART with a 9600 baud rate. If a standard 32.768kHz crystal is used instead, the frequency divider would be 3.4, which would produce an effective baud rate of 9637.65bps. This translates to a maximum error of 17.19%, which is unacceptable for maintaining a stable communication link with the GPS module. This problem is solved by using a 12MHz crystal, which would produce an effective baud rate of 9600bps with 0.00% error with a frequency divider of 1250. The use of a 12MHz crystal does not affect real time keeping nor sampling rate, because a 250Hz signal can be obtained by counting 48,000 cycles of the crystal, and a tenth of a millisecond can be obtained by counting 12,000, both of which fit into a 16bit timer compare register.

Table 3: Component Operating Frequencies

Component	Protocol	Frequency
MCU	-	4, 8, 12, or 16 MHz
ADC	-	200ksps

Component	Protocol	Frequency
Accelerometer	Analog	500Hz
Battery Gauge	I^2C	10-100kHz
Magnetometer	I^2C	0-400kHz
Gyroscope	I^2C	0-400kHz
RF Wakeup	SPI	0-2MHz
SD card	SPI	0-25MHz
GPS	UART	9,600 baud
Xbee	UART	9,600 baud

6.2 Point-to-point communication

This section outlines the minimum requirements for timing signals of the devices connected through GPIO. Table 4 shows the timing requirements for the components. These timing signals do not include forms of serial communication, such as UART, SPI and I^2C. If a device requires a specific setup or hold time, the solution would be to set up a timer and count the specific number of clock ticks that the device requires.

Table 4: Signal Timing Requirements of Components

Signal	Time Required
GPS_DR (DR_INT)	Needs to be toggled by low-high-low with $>$10ms pulse length
GPS_FIX (UI_FIX)	Signal outputs 1s pulse every 2s during valid fix condition
GYR_DR (DRDY/INT2)	Interrupt: enabled until acknowledged by the MCU
MAG_DR (DRDY)	Interrupt: enabled when a new set of measurements are available
RF_WK (WAKE)	Not specified
RFWK_CS (CS)	Needs to be high as long as data needs to be read. 65 clock cycles to calibrate
SD_CD (HCRD_PRST)	Active when card present
SD_CS (CS)	Asserted 74 clock cycles
SU_BERR (!BERR/INT)	Low when error occurs, stays until error is cleared
SU_BUSY (!BUSY)	$>$100ms to complete enumeration/de-enumeration
SU_MODE (MODE)	Active during simple control
XB_DR (!DTR/SLEEP)	Not specified
XB_SLEEP (ON/!SLEEP)	Not specified

6.3 Analog considerations

There is only one analog component in the system, the ADXL377 accelerometer. Care must be taken to ensure that the sampling rate of the MCU's ADC can be set to twice the frequency of the analog signal and that the input voltage range of the ADC is enough to allow for the output voltage swing of the ADXL377. The ADXL377 can output data at a maximum of 1000Hz. This means that the MCU's ADC must be capable of sampling at a rate of at least 2ksps. The MSP430FR5969's ADC is capable of sampling at 200ksps, which is well above the required value. The acceptable input voltage range is specified to be from 0V to +Vcc. Since the ADXL377 output voltage swing ranges from 0.1V to 2.8V, the accelerometer's output can be sampled without suffering from clipping distortion. This makes the ADXL377 compatible with the MCU.

A second consideration should be made when interfacing with an analog component: slew rate compatibility. There is no documented specification of the ADC's slew rate in the MSP430FR5969's data sheet. However, since the output of the accelerometer varies around 6.5 mV/g, the change in amplitude in the input signal should be small enough so that there will not be any slew rate distortion.

7. Memory Usage Details

Figure 4 shows a diagram of the memory used by the software. It is divided into Program Memory (FRAM) and Data (RAM). The values for this diagram were taken from the memory map created by Code Composer Studio. Note that the memory blocks are not drawn to scale.

8. Hardware Reliability and Professional Component

8.1 Design Criteria

The system was designed based on three main criteria: Power and Energy Consumption, Sustainability and Durability, and Data Integrity. Several decisions were made in the design process to accommodate for these three criteria. A discussion of how these criteria were addressed from a hardware perspective follows.

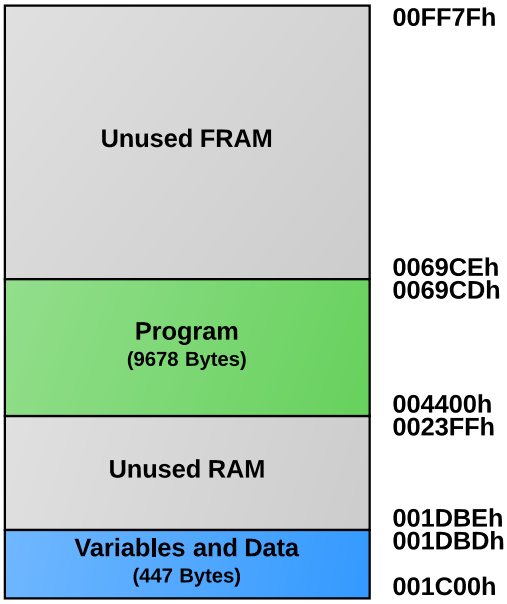

Figure 4: Diagram of the Memory Used By the Software

8.1.1 Power and Energy Consumption

In order to minimize energy consumption, all of the selected ICs have a low-power mode. The only component that does not have a low power mode is the accelerometer, however a power switch was introduced between the power source and the IC which can be controlled via one of the MCU's GPIO pins. This allows for the implementation of a low-power mode for this component.

Another consideration made was in the battery selection. The selected battery has a voltage rating of 3.7V, which is close to the desired power supply voltage of 3.3V. Since the system uses a linear regulator to regulate the power supply at 3.3V, the closer the gap between the battery voltage and the desired power supply, the less energy lost in the regulator as heat.

8.1.2 Sustainability and Durability

Because the drifters are meant to be used in the water, it is important that the plastic casing surrounding the electronic components be durable and able to withstand the large accelerations encountered in the wave-breaking process. At the same time, the internal components must be secured to the casing so that they do not move around inside the plastic casing.

There is currently a Mechanical Engineering student in charge of designing a new plas-

tic casing for the spheres which will later be fabricated for the ongoing NSF funded research project. However, in order to contribute to this criteria, the designed Printed Circuit Boards (PCBs) have holes to allow spacers and screws to fasten the PCB to the casing. This will prevent the PCB from being lose and rattling around inside the casing.

8.1.3 Data Integrity

From a purely hardware perspective, special care was taken when designing the PCB to address this criterion. Antennas were placed according to their specification, which should minimize the chances of data corruption when it is being transmitted wirelessly. In addition, the accelerometer, which is the only analog sensor, was isolated from the rest of the components by placing it on a different ground plane. This reduces the interference that the digital lines will have on the analog lines, which in turn reduces chances of obtaining unreliable measurements from this sensor.

9. System Operation Chart

Operating charts describe the modes of operation and the flow of the system without much detail. Figure 5 shows a state diagram of the system's operation that depicts all available operating. It shows the course of action taken by the software when a complete experiment is performed. A general but brief overview of the different modes of operation follows.

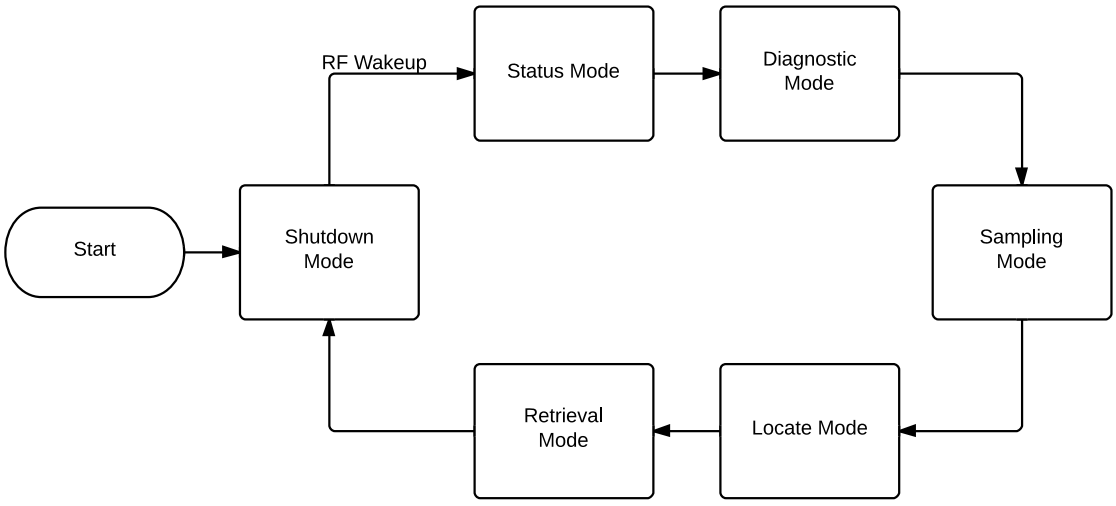

Figure 5: Software state diagram depicting all available operating modes.

When the system is powered up it performs an initialization sequence, which includes initializing all GPIO ports and memory variables. It also enables global interrupts and the

RF wakeup receiver interrupt while keeping all other interrupts disabled. Subsequently all other modules except the RF wakeup receiver are powered down.

Once the initialization sequence is finished, the system enters a very low power mode, called shutdown mode. The system can be woken up by the RF wakeup receiver which is listening for a specific signal from the user. When the system is interrupted from sleep by the RF wakeup receiver it powers on the XBee module, establishes a ZigBee connection, and enables the XBee interrupt. Additionally, the system powers down the RF wakeup receiver and disables its corresponding interrupt.

Afterwards, the system enters another low power mode which is referred to as standby mode. In this mode, the system maintains an active ZigBee connection via the XBee module. At this point, the XBee module is listening for specific signal from the base station. When it receives a signal, it interrupts the MCU and sets a flag corresponding to the signal that was received. The signals received meant are meant to switch between diagnostic, retrieval, sampling, status, locate or shutdown mode. A signal can also tell the drifters to exit diagnostic mode or to exit locate mode. The interrupt routine then takes the CPU to active mode, and the system proceeds to execute the service corresponding to the signal that was sent to the XBee module via the base station. After the service has finished executing, the system returns to standby mode where it listens for more incoming commands.

10. Software Organization

The software in the system is composed of two parts: the software embedded in the drifters and the application GUI in the base station. A description of how the software is organized follows.

The drifters contain the embedded software which the MCU runs. It is developed in C language and is the same for all drifters. The GUI that resides on the base station was developed in Java and libraries were used to establish serial communication with the Xbee.

In order for the base station to manage multiple drifters, a unique ID is given to each of them. A protocol not dissimilar to I^2C was implemented in order to manage the communication between the spheres: the Base Station acts as a master and the drifters act as the slaves. Whenever the base station needs to write or read data from the drifters, it issues a command by first sending the address of the drifter and then sending the command to be interpreted by the drifter. When writing data to the drifters, only the command is sent, since writing data in this case means sending a single command to change the operating mode of the drifter. When reading data, the address and command of the drifter from which it is intended to read are broadcasted. Once the drifter has received its own address, it takes control of the communication with the base station and begins transmitting the requested data.

11. Software Reliability and Professional Component

11.1 Design Criteria

As previously mentioned, the system was designed based on three main criteria: Power and Energy Consumption, Sustainability and Durability, and Data Integrity. Several decisions were made in the design process to accommodate for these three criteria. A discussion of how these criteria were addressed from a software perspective follows.

11.1.1 Power and Energy Consumption

In order to minimize energy consumption, the software was written to be interrupt driven. Whenever the microprocessor is idle or is not performing a time-critical task, it is sent into one of the available power modes. This dramatically lowers the current drawn from the power supply, which in turn extends the battery life.

11.1.2 Sustainability and Durability

From a purely software perspective, there is little that can be done to address the sustainability and durability criterion since the software is not capable of changing the physical aspects of the system.

11.1.3 Data Integrity

Currently, the only measure for addressing this criterion in the software is configuring the MCU's analog-to-digital converter to oversample the output of the accelerometer and take an average of these samples so as to create some type of filter for noise. Since noise is a random phenomenon, sampling the accelerometer output once for a single data point could lead to a noisy measurement. These chances are reduced when an average of 16-32 samples are taken as a single data point.

Aside from this, the UART peripheral in the MCU was configured so that there would be a 0% error in the 9600 baud rate. This also contributes to data integrity since minimizing error in this form of asynchronous serial communication will undoubtedly minimize the chances of data getting corrupted when they are being transmitted.

12. System Limitations

12.1 Hardware Limitations

During the late stages of the prototype development one of the researchers discovered from his gathered data that the gyroscope was very sensible to vibrations and changes in acceleration, something that will always occur because of the nature of the experiments being conducted with these drifters. The gyroscope used for this prototype suffers from the same negative effect as the one the researcher is using. Because of the advanced stage of development, it became unfeasible to change the selected gyroscope to one that was more resistant to these effects. Therefore, in a future version of the prototype a new gyroscope that is shock resistant needs to be chosen in order to yield better results.

12.2 Software Limitations

Due to the time constraints imposed on the project, at the time this work was published, one of the biggest limitations in terms of software is the inability to calibrate the sensors without having to re-compile the code. The effect of sensor calibration is seen when the raw data obtained from the sensors is converted into real data with physical meaning. For each measurement, a minimum of scaling and offset factors should be included and are currently not present. This has also been recommended as a possible extension of the software in Section 14. However, since sensor calibration can be different between board to board due to the stress and strain caused when the surface-mounted components are soldered, it can be argued that it is best for the system to save and manage raw data. This data can later be converted into physical values by a separate data analysis software that can take the calibration parameters as input.

13. Conclusion

The proposed 7.5cm drifter was successfully designed and implemented. The space constraint, which proved to be the most prohibitive and difficult to adhere to constraint was satisfied by introducing a two-tiered printed circuit board (PCB) structure consisting of two individual PCBs connected through a board-to-board connector. The newly introduced components solve certain problems that had been previously encountered by the researchers. For example, the on-board GPS solves the problem of the drifters getting lost at sea with no way to locate them, while the RF wakeup module solves the water leakage problem introduced when attempting to mount an external push button to activate the sphere. From a data collecting perspective, a faster and steady sampling rate was achieved (250Hz) in comparison to the existing prototype being used by the researchers.

An application in the form of a Graphical User Interface (GUI) was successfully implemented and tested. This allows the researchers to manage the drifters as mentioned throughout this work. Capabilities for managing multiple drifters at the same time were implemented and are available for the users.

14. Future Work

The calibration of the sensors can be different from board to board because of the different amounts of stress caused by the soldering process. Since data conversion takes place in the Graphical User Interface this means that a calibration mode should be added to the software. The software should take at least two parameters for each sensor axis: a scaling factor and an offset. Although there are very elaborated calibration processes and methods, these two parameters are essential to any calibration process.

From a software perspective, more measures to protect data integrity should be implemented since for this type of application having corrupted data is unacceptable. Some measures might include storing data redundantly, oversampling and averaging values on other sensors, among others.

From a hardware perspective, a shock-resistant gyroscope should replace the one used in the current design. The battery meter is yet to be fully connected and the software needed to communicate with this component is yet to be fully implemented. This component has been included throughout the design process but since it is not a system critical component, it has not been completely integrated at the time this work was published. In addition to this, since the first level PCB has not arrived from the fabrication company at the time this work was published, all components still need to be soldered on to the board and tested. The second level PCB arrived shortly before the deadline imposed on this work and therefore all components still need to be soldered as well.

15. Acknowledgements

The authors of this work would like to thank Dr. Miguel F. Canals and Andre Amador for the idea for this project and their support, both technical and financial, throughout this project. This project is based on the graduate research done by Andre Amador and the design of this device is based on the ideas presented in [4]. Funding for this project was provided by Dr. Miguel F. Canals.

The authors would also like to thank Dr. Manuel Jiménez for his technical feedback and advice throughout this semester.

16. References

[1] "BoaterExam." http://www.boaterexam.com/usa/michigan/education/?chapter=6&page=9.

[2] A. Amador, "Lagrangian observations of turbulence in breaking surface waves." 2012.

[3] R. Granger, *Fluid mechanics*. Dover Books on Physics Series, Dover Publications, Incorporated, 1985.

[4] A. Amador, M. Canals, G. Guerrero, J. Cruz, and E. Ortiz, "Development of novel instrumented lagrangian drifters to probe the internal structure of breaking surface waves," in *Oceans, 2012*, pp. 1 –6, oct. 2012.

[5] R. Jirawimut, P. Ptasinski, V. Garaj, F. Cecelja, and W. Balachandran, "A method for dead reckoning parameter correction in pedestrian navigation system," in *Instrumentation and Measurement Technology Conference, 2001. IMTC 2001. Proceedings of the 18th IEEE*, vol. 3, pp. 1554–1558 vol.3, 2001.

[6] "The I^2C-Bus Specification." http://www.nxp.com/documents/other/39340011.pdf.

[7] D. Ibrahim, *SD Card Projects Using the PIC Microcontroller*. IT Pro, Elsevier Science, 2010.

[8] M. Jiménez, R. Palomera, and I. Couvertier, *Introduction to Embedded Systems: Using Microcontrollers and the MSP430*. Springer London, Limited, 2013.

Appendix A: User's Guide

This section contains a guide with instructions on how to operate the drifters. It also describes the capabilities of the Graphical User Interface (GUI) and how it interacts with the drifters.

User guide

Contents

Setup

WaveSphere consists of two parts: the spheres (drifters) and the base station (computer). The spheres need to have their batteries charged in order for the system to operate properly. In order to use the system, first plug the Xbee Explorer dongle into the base station computer. Once connected, you can proceed to run WaveSphere.jar. When the GUI opens, the first window that appears looks like the one shown in **Figure 1**. You will need to select, from the list, the port associated with the Xbee.

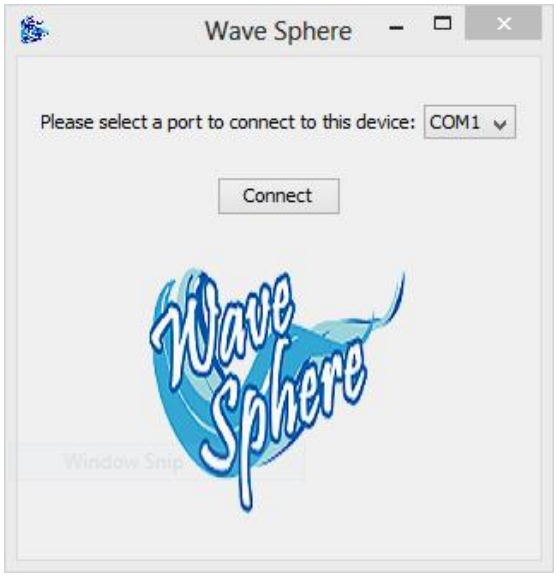

Figure 1: Main Window

After getting connected, you will see a window like the one shown in **Figure 2**. You need to add the spheres you will use for this experiment in order to proceed. Press the Add New Sphere button to proceed.

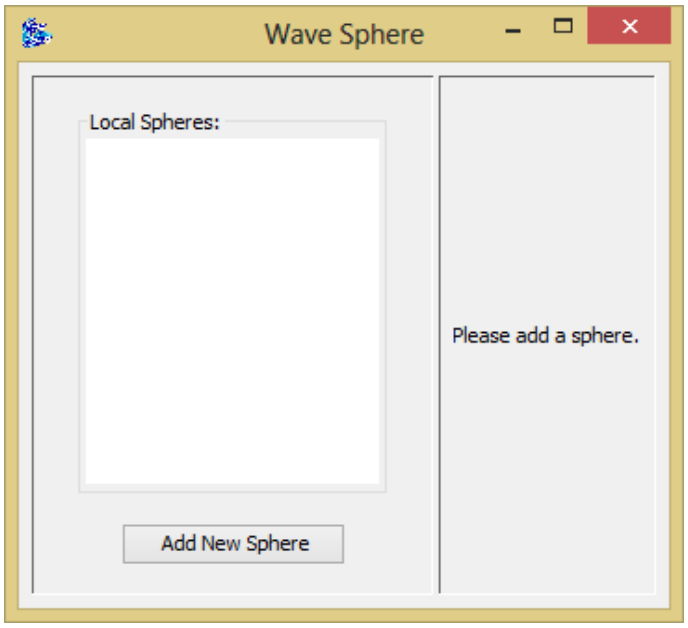

Figure 2: Window without spheres

After clicking the Add New Sphere button, a form for adding a new sphere, like the one shown in **Figure 3**, appears. The ID needs to be in the form XXX-XXXX, where Xs are one digit numbers (0-9) and the name can be any string, as shown in **Figure 4**. You can continue adding spheres until you press cancel.

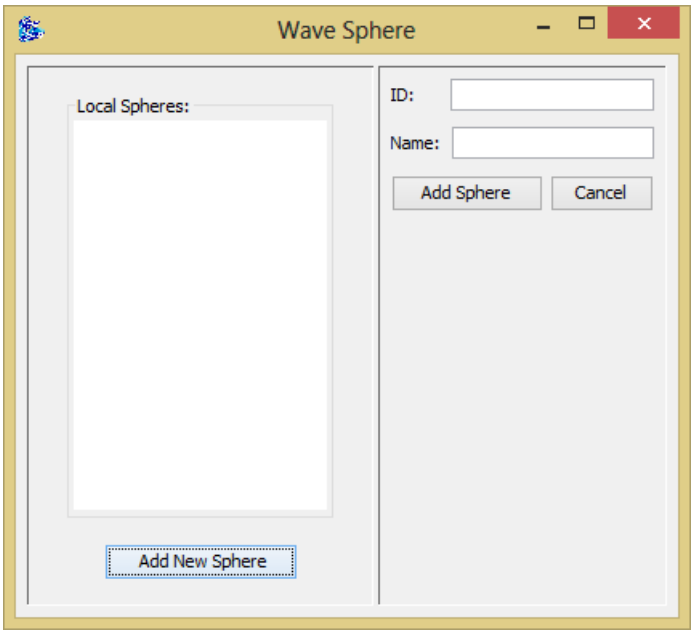

Figure 3: Add New Sphere blank

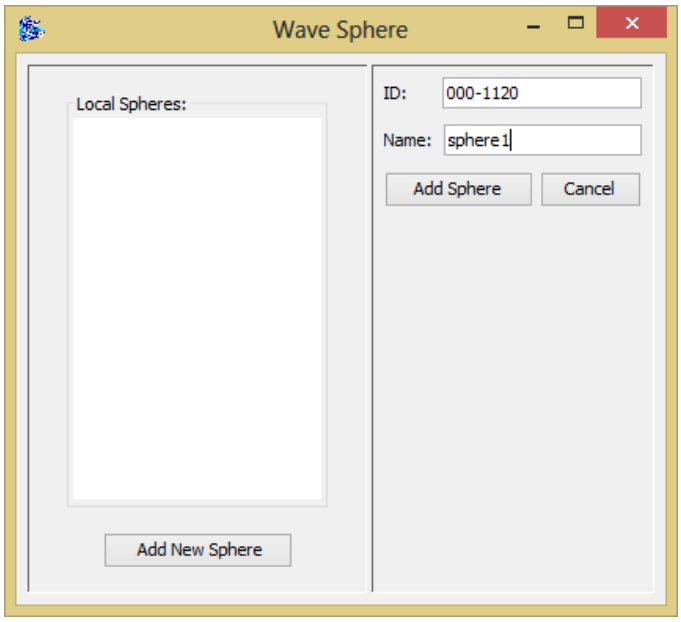

Figure 4: Add New Sphere Example

After adding the sphere, it will appear in the list on the left, as shown in Figure 5.

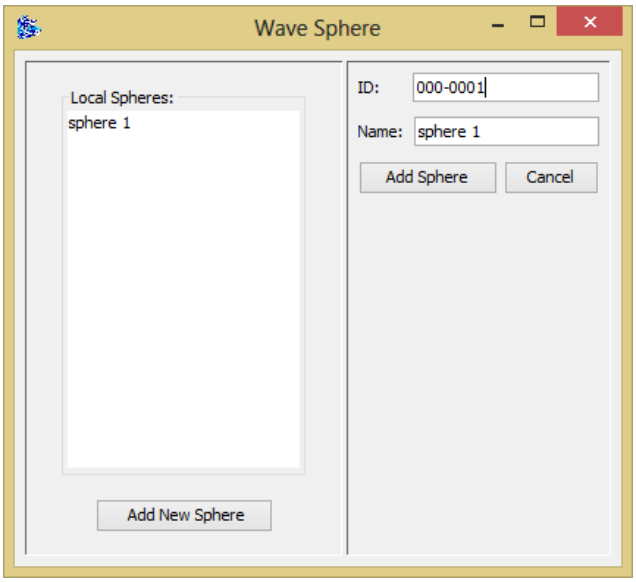

Figure 5: Window with added spheres

In order to manage a sphere, you need to select one from the list. Then you can proceed to initiate the different modes (retrieval, sampling, diagnostic or shutdown). Make sure you have turned on the desired sphere by passing the RFID reader to the sphere. If you fail to do so, the GUI will not work properly.

Operation

Retrieval Mode

When Retrieval Mode is selected, a save dialog appears (as shown in **Figure 6**). You will need to select a location and a name for your text file (make sure to include the desired extension: .txt for example).

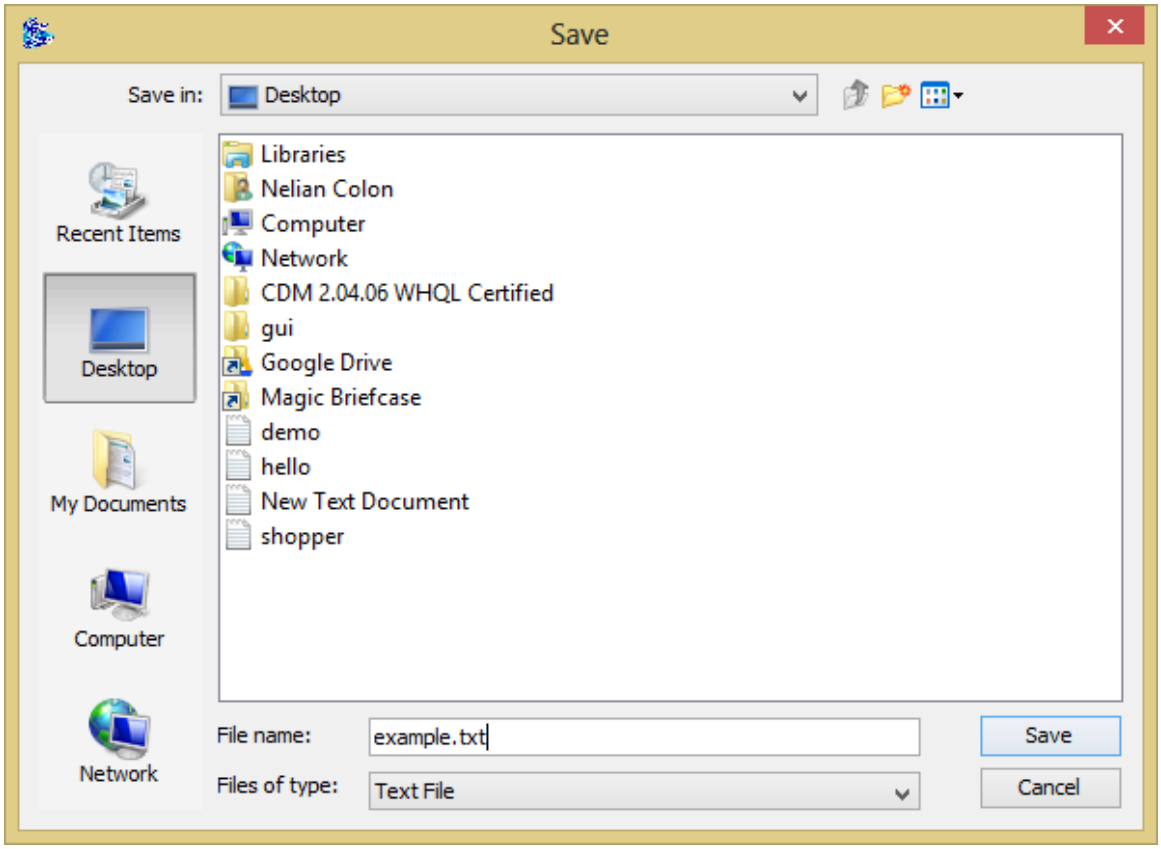

Figure 6: Save Dialog - Retrieval Mode

Do not proceed until you see a dialog stating that the file was saved, as shown in **Figure 7**. Otherwise, data will be corrupted.

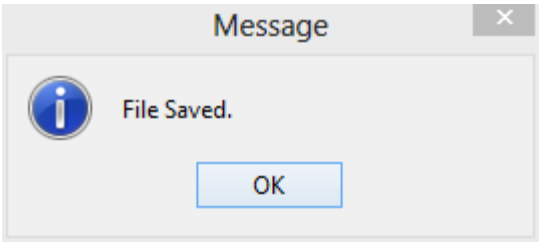

Figure 7: File Saved

Sampling Mode

When sampling mode is selected, the GUI will enter into a waiting screen as shown in **Figure 8**.

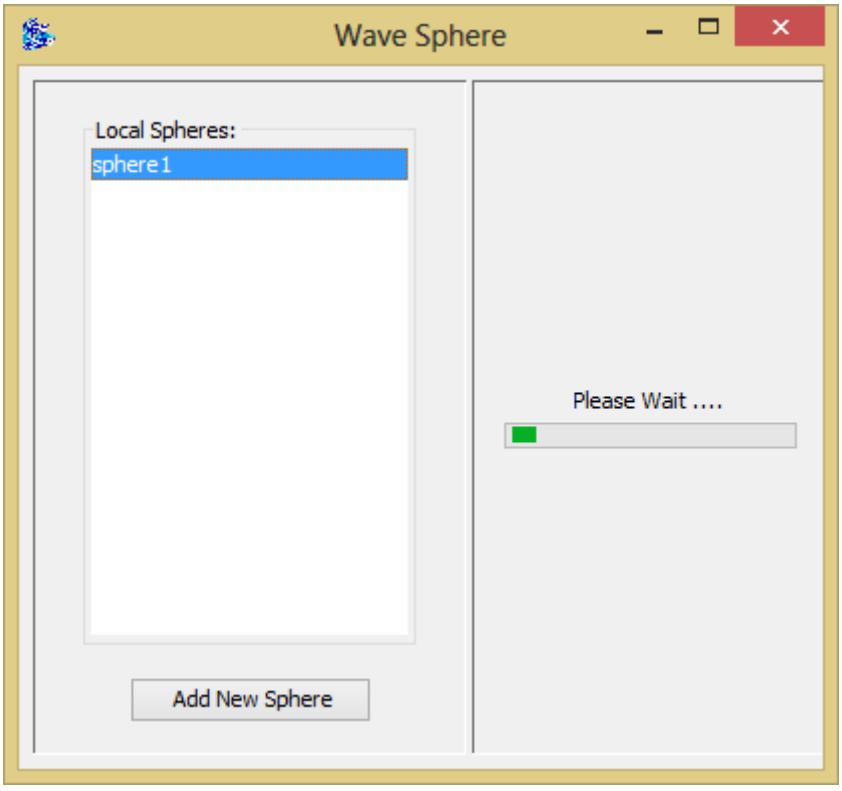

Figure 8: Sampling Mode

Locate Mode

After finishing sampling, you can proceed to locate your sphere. Locate mode will look as the one shown in **Figure 9**.

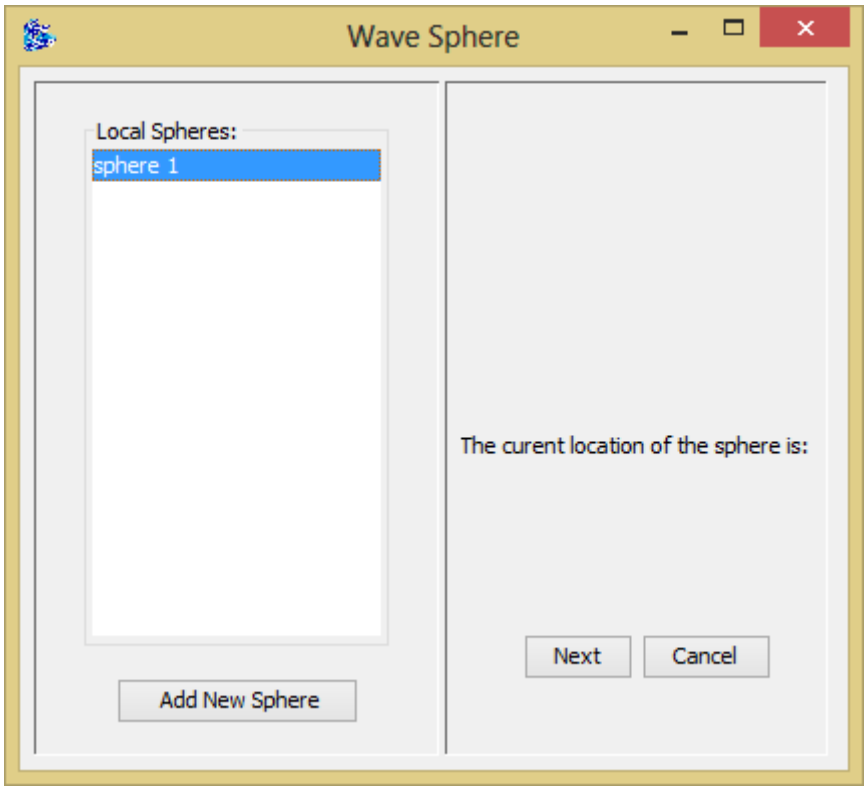

Figure 9: Locate Mode

Location will be shown until the exit button is pressed or until the next button after the last sphere's location has been shown.

Diagnostic Mode

When the diagnostic mode is selected, the right panel changes into diagnostic mode. **Figure 10** shows how it looks like.

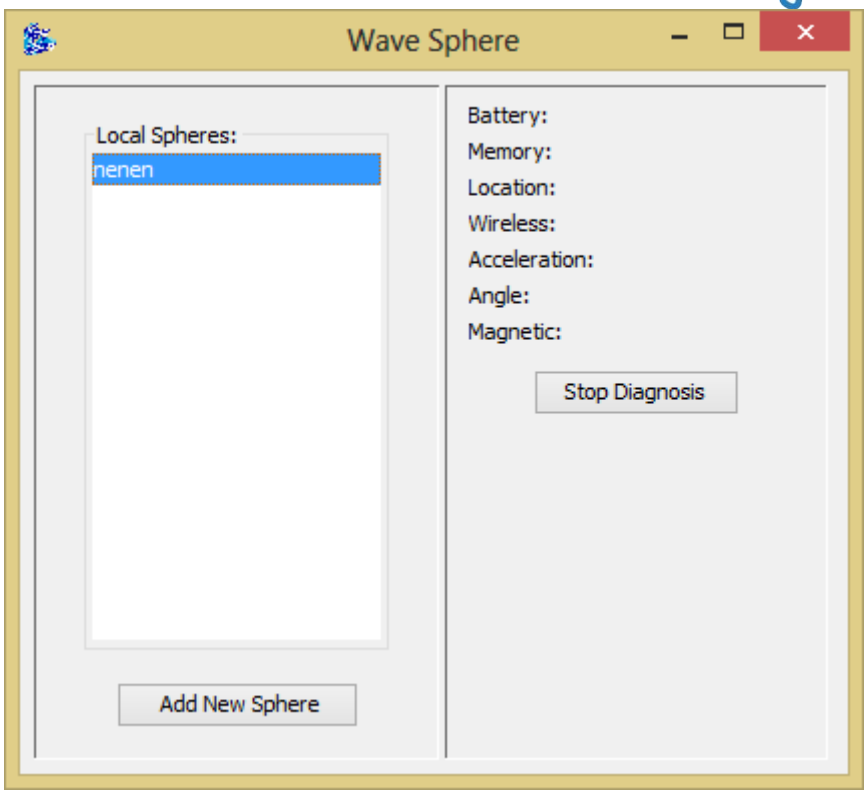

Figure 10: Diagnostic Mode

Status Mode

Whenever a sphere is selected and exits from other mode (Sampling, Retrieval, Diagnostic or Locate), the GUI will enter in Status Mode. Status Mode, as shown in **Figure 11**, shows the ID of the selected sphere, the memory available and the battery level.

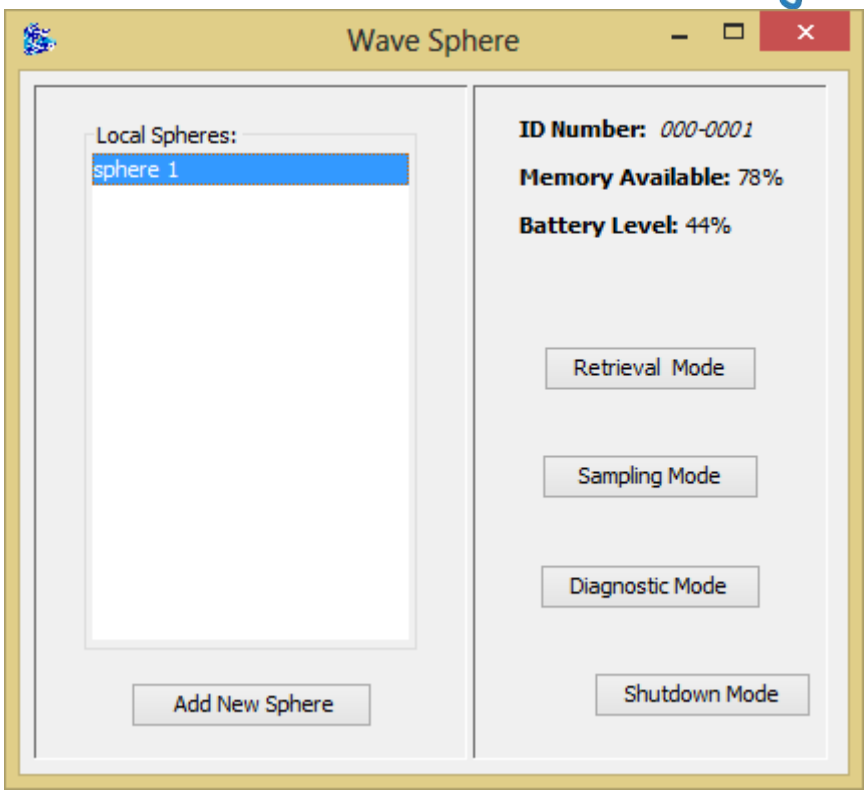

Figure 11: Status Mode

Appendix B: System Schematics

This appendix contains the schematics for the system.

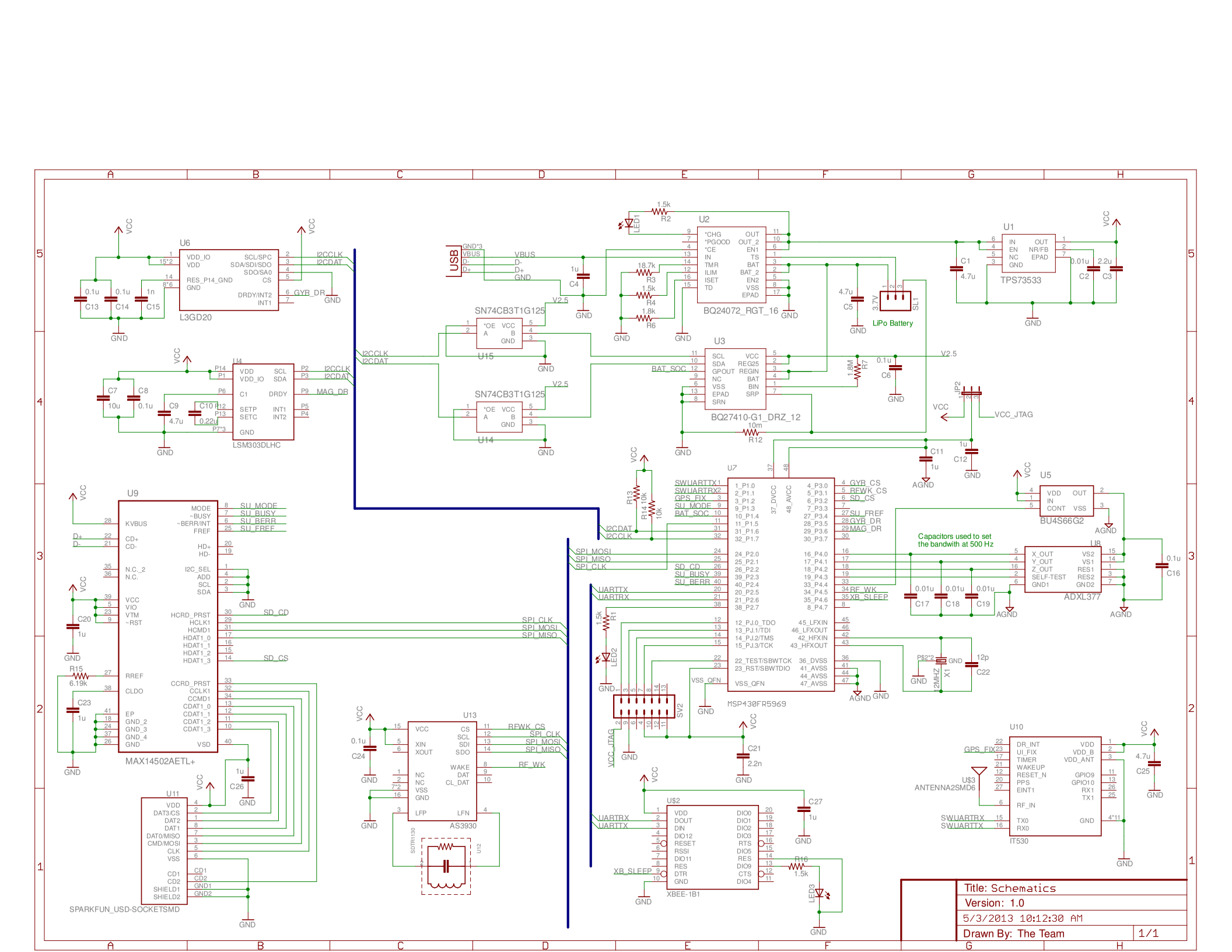
U6
L3GD20
U4
LSM303DLHC
U15
SN74CB3T1G125
U14
SN74CB3T1G125
U2
BQ24072_RGT_16
U3
BQ27410-G1_DRZ_12
U1
TPS73533
LiPo Battery
USB
U9
MAX14502AETL+
U11
SPARKFUN_USD-SOCKETSMD
U13
AS3930
U7
MSP430FR5969
U5
BU4S66G2
U8
ADXL377
U10
IT530
U$3
ANTENNA2SMD6
U$2
XBEE-1B1
SV2
JP2
VCC_JTAG
Capacitors used to set the bandwith at 500 Hz
I2CCLK
I2CDAT
SPI_MOSI
SPI_MISO
SPI_CLK
SD_CD
SD_CS
RF_WK
REWK_CS
GYB_DR
MAG_DR
UARTTX
UARTRX
XB_SLEEP
SWUARTRX
SWUARTTX
GPS_FIX
VCC
GND
AGND
Title: Schematics
Version: 1.0
5/3/2013 10:12:30 AM
Drawn By: The Team
1/1

Appendix C: Component Layout

This section contains the diagrams of the designed Printed Circuit Boards. In the diagrams shown, the component placement can be seen. The reference numbers displayed on the PCB layout are the same that are found in the first and second level schematics that accompany the boards.

Recall that the PCB was designed with two levels. Figure 6 and 7 show the schematic and board layout for the first level of the PCB respectively. In the same manner, Figure 8 and 9 show the schematic and board layout for the second level.

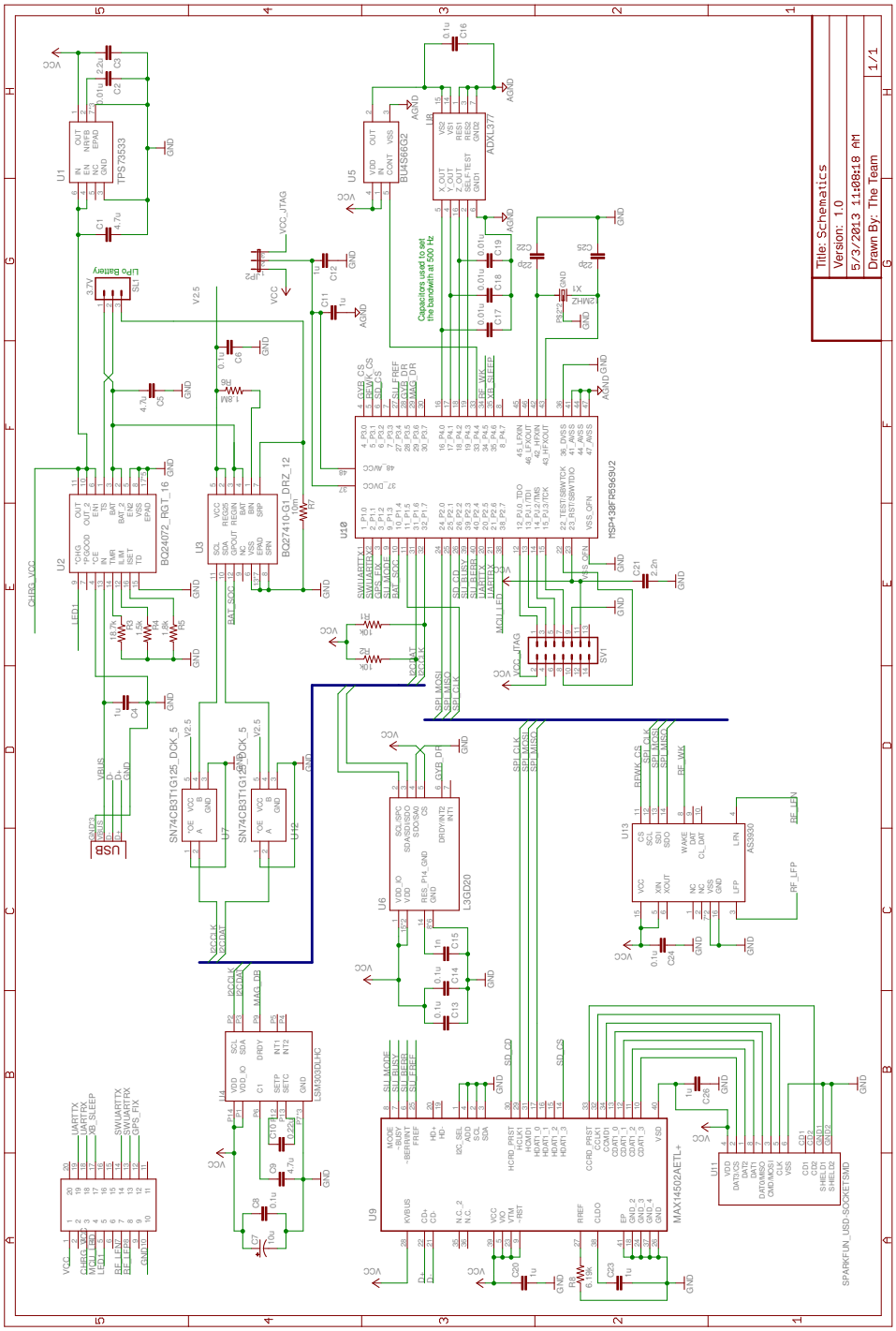

Figure 6: Schematic for First Level of PCB

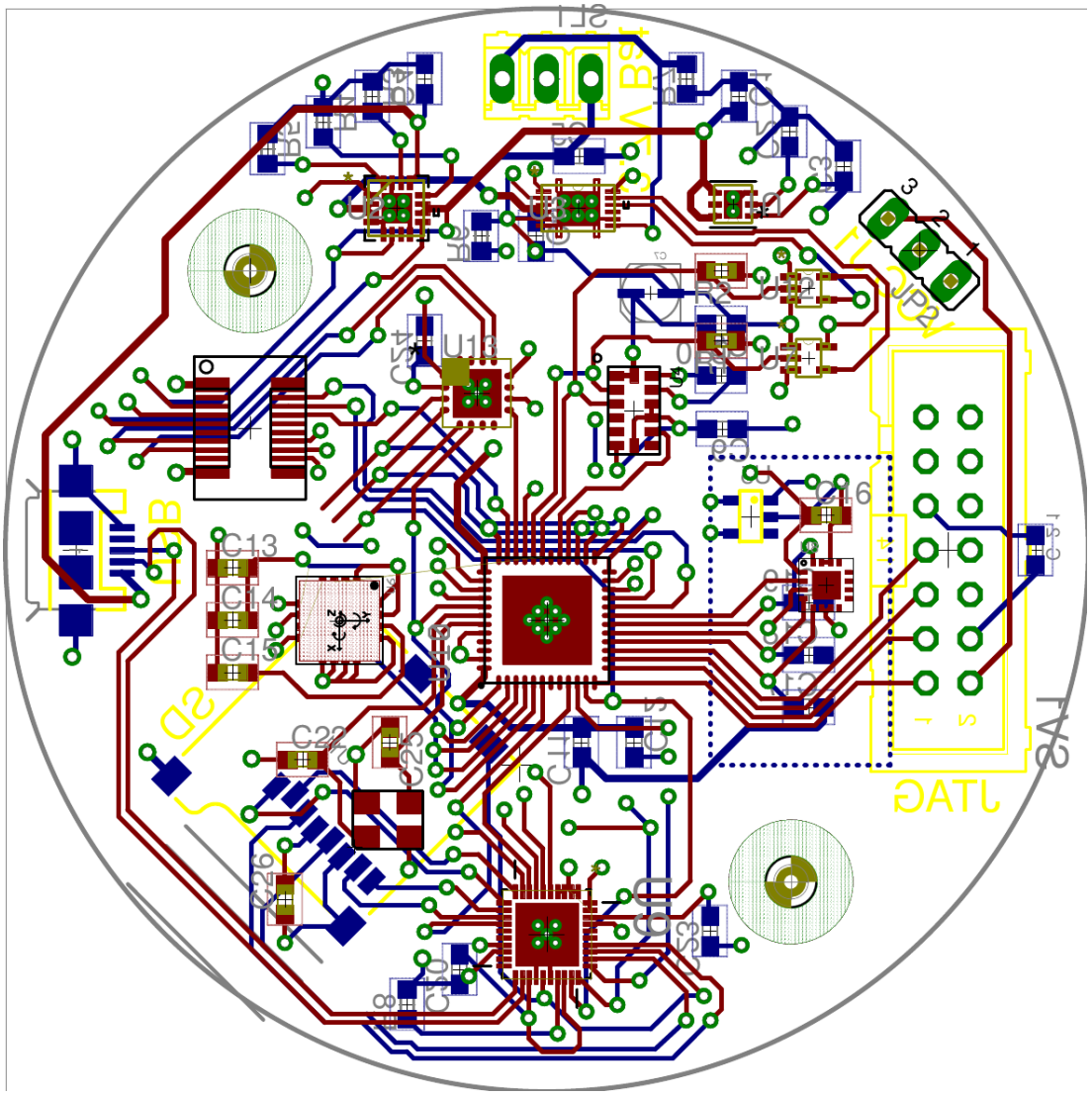

Figure 7: Schematic for First Level of PCB

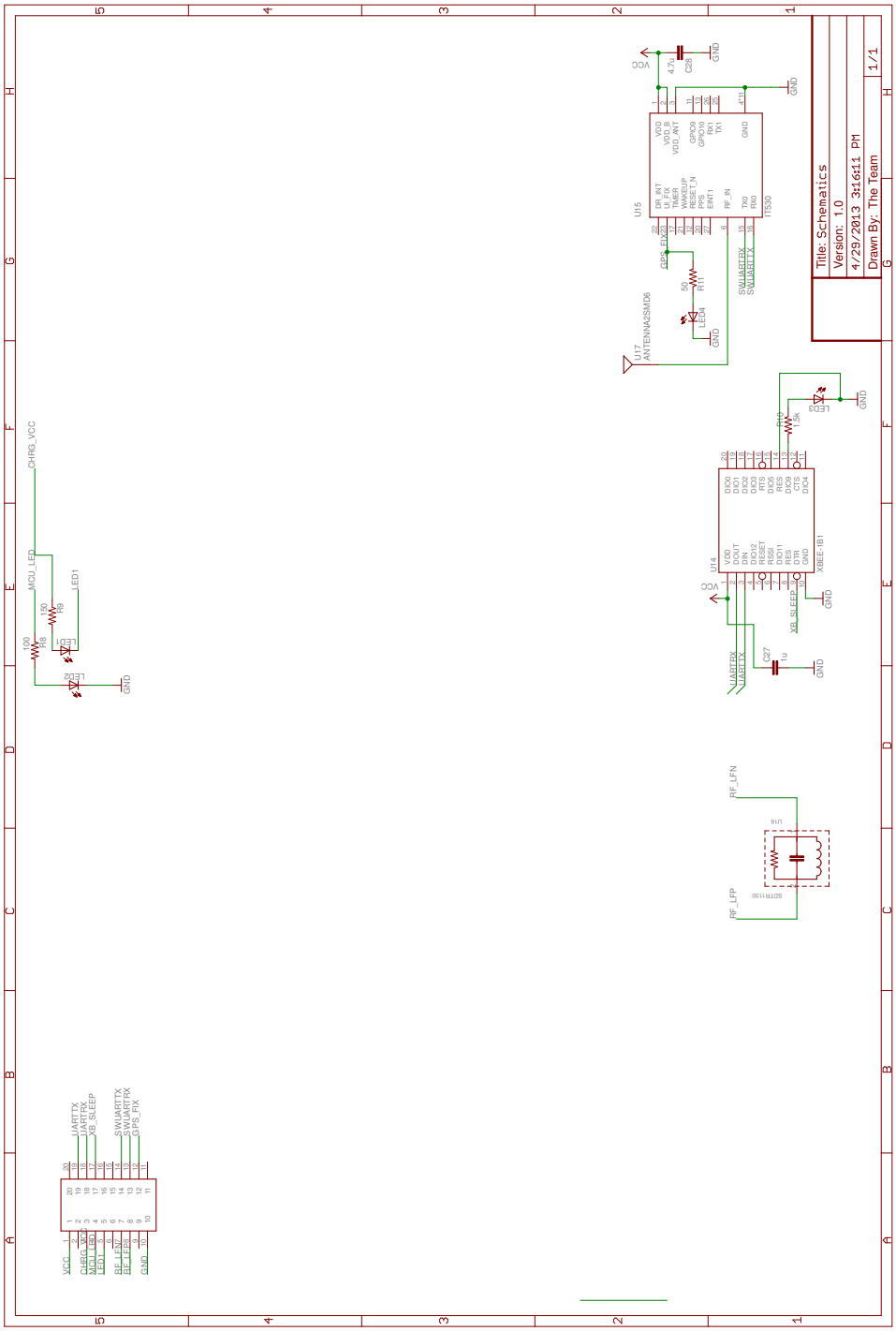

Figure 8: Schematic for First Level of PCB

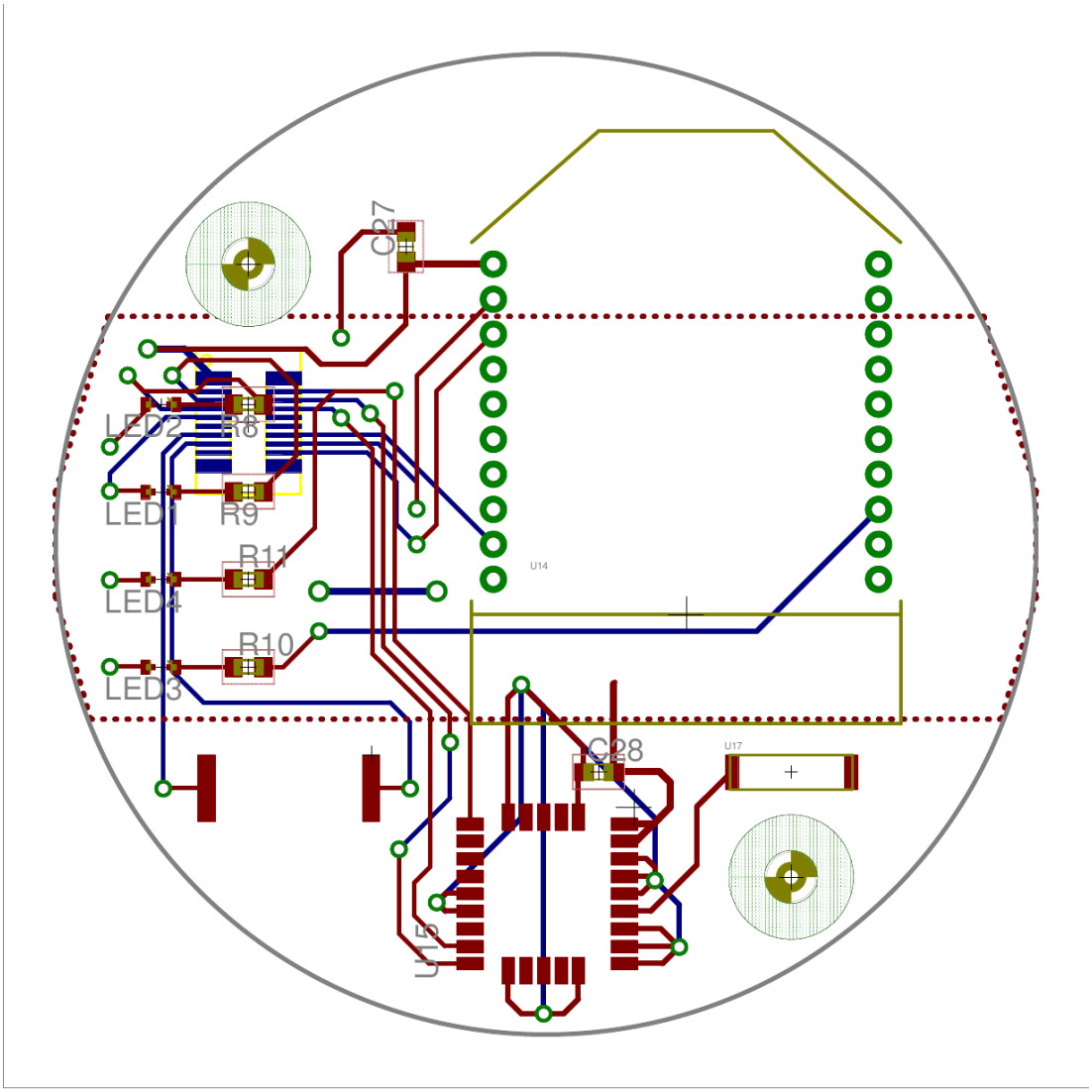

Figure 9: Schematic for First Level of PCB

Appendix D: Extended Power Analysis

This section contains a more detailed explanation of how the battery life was estimated. It includes the assumptions made to generate the activity factors. In addition, it includes a thorough description of the calculations made in the thermal analysis.

D.1 Battery Life Estimate

In order to estimate the battery life, the average supply current was determined by using a weighted average based on the fraction of time each component is active. The weighted average formula used was: $I_{avg} = \alpha * I_{active} + (1-\alpha) * I_{LPM}$, where α is the activity factor or the fraction of time the component is active. The following assumptions were made when determining the activity factor.

- The drifters will spend 10 minutes in "Locate Mode" before they are retrieved from the water.
- The drifters will spend 30 seconds in sampling mode.
- The drifters will spend 3 minutes in stand-by mode before they are deployed.
- The drifters will spend about 10 seconds transferring a single data file. The following assumptions were made to determine this time:
  - File Size: 200 kB * 8 = 16,000 kbits.
  - 80% of XBee maximum Speed: 250 kbps * 80% = 200 kbps.
  - 16,000 kbits / 200 kbps = 8 seconds, which can be rounded up to 10 seconds.

Table 5 shows a list of the components along with their active and low power mode supply current, determined activity factor, and weighted average supply current. It also shows the total average current consumption of the system which was determined to be around 70 mA. This means that a chosen 500 mAh battery will last for about 7.23 hours. Based on the current assumptions, a single throw or experiment will last for about 13.66 minutes, which means that the drifters will be able to perform at least 30 experiment trials under the current assumptions.

Table 5: Activity Factors Used to Estimate Battery Life

Component	I_{Active} (μA)	I_{LPM} (μA)	α	I_{AVG} (μA)
Connected To LDO				
MSP430FR5969	1600	0.5	78.05%	1248.91
3-Axis Accelerometer	300	0	3.66%	10.98
Magnetometer	110	1	3.66%	4.9894
XBee	45000	0.5	96.34%	43353.02
RF Wakeup	2.7	0.4	0.00%	0.4
Gyroscope	6100	5	3.66%	228.077
GPS	26140	5	73.17%	19127.98
SD Card	100000	10	4.88%	4889.512
Power switch	1	0.3	3.66%	0.32562
SD to USB	37	1	100.00%	37
Connected Directly to Battery				
LDO	65	1	100.00%	65

Component	I_{Active} (μA)	I_{LPM} (μA)	α	I_{AVG} (μA)
Battery Charger	1500	6.5	0.00%	6.5
Battery Meter	103	4	100.00%	103
Total	180958.7	35.2	-	69075.69
Battery Capacity	500 mAh	Hours of Use per charge		7.238436
Est. time per throw (min)	13.66 mins	Throws per charge		31.7785

D.2 Thermal Analysis

Performing a thermal analysis on the system will reveal whether the operating temperature of the individual ICs is below their maximum rating. In order to perform this analysis, the junction temperature T_J will be calculated for the MCU and the power management ICs. The junction temperature is given by [8, 419]:

$$T_J = T_A + \theta_{JA} \cdot P_{diss}$$

where T_J is the estimated junction temperature, T_A is the ambient temperature (taken here to be $27^{\circ}C$), θ_{JA} is the junction-to-ambient thermal resistance and P_{diss} is the estimated power consumption of the device.

This formula is applied throughout the following sections to determine whether the MCU and the power ICs will be operating at a safe temperature or if they require additional heat dissipation mechanisms such as heat syncs, fans, etc.

D.2.1 Microcontroller

In order to estimate the average operating junction temperature for the MCU the power dissipated by the IC will first be calculated. The following formula, which was taken from [8, 419], will be used:

$$P_{diss} = V_{DD} \cdot \left(I_{DD(avg)} + \sum_{allpins} |I_{IO(avg)}| \right)$$

Although no information is available for the θ_{JA} of the MSP430FR5969, since this value depends on the package and the area exposed to the air, a device with the same package (48-pin QFN), the MSP430F5510, was found to have $\theta_{JA} = 28.6^{\circ}C/W$ and this value was

instead used. In the same manner, although no information on the IO currents is available, the ones for the MSP430F5510 will be used instead.

In full drive mode, the MSP430F5510 can output upto 45mA through its IO pins while still maintaining a valid V_{OL}. Table 6 shows the assumed IO currents for each components.

Table 6: Worst Case I/O current for microcontroller pins

Pin	$I_{DD(Active)}$ (μA)	Qty	Total Current (μA)
SPI	100	3	300
I^2C	10	2	20
UART	1000	2	2000
GPIO	1000	21	21000
		Total	23320

Assuming an IO current of 23.32mA and an average supply current of 1.6mA, the total power dissipation can then be calculated to be:

$$P_{diss} = V_{DD} \cdot (1.6m + 23.32m)$$

$$\boxed{P_{diss} = 82.24mW}$$

Using $\theta_{JA} = 47.8^{\circ}C/W$, the total junction temperature is then given by:

$$T_J = 27 + 26.8 \cdot 0.08224$$

$$\boxed{T_J = 29.20^{\circ}C}$$

The datasheet states that the maximum junction temperature is $95^{\circ}C$, which means that in this application, the device is well under the maximum operating temperature rating and no additional heat dissipation mechanism is needed.

D.2.2 Low-Dropout Regulator

The datasheet for the TPS73501 contains a section on power dissipation and provides the following formula for calculating the power dissipation across the device:

$$P_{diss} = (V_{IN} - V_{OUT}) \cdot I_{OUT}$$

The voltage provided by the battery charger circuit is 3.925 V and the required output voltage is 3.3 V. The estimated output current required is 180.96 mA. In order to leave a

margin of error, a rounded value of 200 mA will be used in this calculation. Thus, the power dissipated by the device is given by:

$$P_{diss} = (3.925 - 3.3) \cdot 200m$$
$$\boxed{P_{diss} = 125mW = 0.125W}$$

Since for this device, $\theta_{JA} = 47.8°C/W$, the total junction temperature is then given by:

$$T_J = 27 + 47.8 \cdot 0.125$$
$$\boxed{T_J = 32.98°C}$$

The datasheet states that the maximum junction temperature is $150°C$, which means that in this application, the device is well under the maximum operating temperature rating and no additional heat dissipation mechanism is needed.

D.2.3 Battery Charger

The datasheet for the BQ24072 provides the following formula for estimating the power dissipation across the device.

$$P_{diss} = (V_{IN} - V_{OUT}) \cdot I_{OUT} + (V_{OUT} - V_{BAT}) \cdot I_{BAT}$$

The output voltage of the device is 5.5 V, while the input voltage is 5 V as dictated by the USB standard. The output current can be estimated to be 50mA by taking into account the two LEDs connected to this pin (at about 20mA per LED) and the LDO input (46 μA) and rounding up to leave a margin for safety. The circuit was designed for a battery voltage of 3.7 V and a current of 800 mA.

$$P_{diss} = (5 - 3.925) \cdot 50m + (3.925 - 3.7) \cdot 500m$$
$$\boxed{P_{diss} = 166mW}$$

Since for this device, $\theta_{JA} = 39.47°C/W$, the total junction temperature is then given by:

$$T_J = 27 + 39.47 \cdot 0.166$$
$$\boxed{T_J = 33.55°C}$$

The datasheet states that the maximum junction temperature is $125°C$, which means that in this application, the device is well under the maximum operating temperature rating and no additional heat dissipation mechanism is needed.

D.2.4 Battery Meter

Although the datasheet for the BQ27410 does not provide a direct formula for power dissipation and because the battery meter has an internal LDO, the formula used for the MCU IO pins will be combined with the power dissipation formula of the LDO to obtain a more robust estimate for the power dissipated.

$$P_{diss} = V_{DD} \cdot \left(\sum_{all pins} |I_{IO(avg)}| \right) + (V_{IN} - V_{OUT}) \cdot I_{OUT}$$

The IO pin output current for this device is between 0.5 and 1 mA. 1 mA will be used for the two I^2C pins, which gives a total IO current of 2 mA. The maximum supply current is 103 μA and this will be used instead of the average supply current to leave a margin of safety. The input voltage is 5.5 V and the regulated output voltage is 2.5 V.

$$P_{diss} = 2.5 \cdot (2m) + (3.7 - 2.5) \cdot 0.103m$$

$$\boxed{P_{diss} = 5.12mW}$$

Since for this device, $\theta_{JA} = 64.17°C/W$, the total junction temperature is then given by:

$$T_J = 27 + 64.1 \cdot 0.00512$$

$$\boxed{T_J = 27.33°C}$$

The datasheet states that the maximum junction temperature is $100°C$, which means that in this application, the device is well under the maximum operating temperature rating and no additional heat dissipation mechanism is needed.

Appendix E: Bill of Materials

This section contains a list of the essential components needed for this project.

Table 7: Bill of Materials

Part	Manufacturer	Mfg #	Distributor	Price	Qty	Total
12MHz Crystal	Epson Toyocom	FA-238V	Mouser	$3.75	1	$3.75
3-pin JST Connector			Sparkfun	$0.95	1	$0.95
Accelerometer	Analog Devices Inc	ADXL377BCPZ-RL7	Digi-Key	$11.12	1	$11.12
Amber LED	Panasonic Electronic Components	LNJ426W83RA	Mouser	$0.46	1	$0.46
Battery Charger	Texas Instruments	BQ24072RGTT	TI	$2.98	1	$2.98
Battery Meter	Texas Instruments	BQ27410DRZT-G1	TI	$4.28	1	$4.28
Blue LED	Harvatek International	HT-F199NB5-5490	Mouser	$0.35	1	$0.35
Board to Board Connector Header	Panasonic Electric Works	AXK6S20547YG	Digikey	$1.53	1	$1.53
Board to Board Connector Socket	Panasonic Electric Works	AXK5S20347YG	Digikey	$1.53	1	$1.53
Capacitor, 0.01u	Kemet	C0603C103K3GACTU	Mouser	$0.35	4	$1.40
Capacitor, 0.1u	Taiyo Yuden	EMK107B7104KA-T	Mouser	$0.09	6	$0.54
Capacitor, 0.22u	Taiyo Yuden	LMK107B7224KA-T	Mouser	$0.20	1	$0.20
Capacitor, 10u	Cornell Dubilier	AVE106M16A12T-F	Mouser	$0.14	1	$0.14
Capacitor, 1n	Kemet	C0603C102J5GACTU	Mouser	$0.10	1	$0.10
Capacitor, 1u	Taiyo Yuden	LMK107BJ105KA-T	Mouser	$0.21	7	$1.47
Capacitor, 2.2n	Kemet	C0603C222J5GACTU	Mouser	$0.30	1	$0.30
Capacitor, 2.2u	Taiyo Yuden	LMK107BJ225KA-T	Mouser	$0.30	1	$0.30
Capacitor, 22p	Taiyo Yuden	UMK063CG220JT-F	Mouser	$0.20	2	$0.40
Capacitor, 4.7u	Taiyo Yuden	JMK107BJ475KA-T	Mouser	$0.39	4	$1.56
GPS	Fastrax	IT530	Mouser	$32.50	1	$32.50
GPS Antenna	Johanson Technology	1575AT43A0040	Sparkfun	$1.50	1	$1.50
Green LED	Lite-On	LTST-C193KGKT-5A	Mouser	$0.10	1	$0.10
Gyroscope	STMicroelectronics	L3GD20	Mouser	$6.76	1	$6.76
JTAG Socket	3M	2514-6002UB	Digikey	$2.57	1	$2.57
LDO	Texas Instruments	TPS73533DRVT	TI	$1.87	1	$1.87
Level Shifters	Texas Instruments	SN74CB3T1G125DCKR	Mouser	$1.04	2	$2.08

Part	Manufacturer	Mfg #	Distributor	Price	Qty	Total
Magnetometer	STMicroelectronics	LSM303DLHC	Mouser	$4.89	1	$4.89
Microcontroller	Texas Instruments	XMS430FR5969IRGZR	TI	$4.19	1	$4.19
microSD card socket			Sparkfun	$3.95	1	$3.95
microUSB Port			Sparkfun	$1.50	1	$1.50
Power Switch For Accelerometer	Rohm Semiconductor	BU4S66G2-TR	Digi-Key	$0.63	1	$0.63
Red LED	Harvatek International	HT-F199USD5-5493	Mouser	$0.40	1	$0.40
Resistor, 1.5k	Bourns	CR0603-JW-152GLF	Mouser	$0.20	1	$0.20
Resistor, 1.8k	Bourns	CR0603-JW-182ELF	Mouser	$0.06	1	$0.06
Resistor, 1.8M	Bourns	CR0603-JW-185ELF	Mouser	$0.09	1	$0.09
Resistor, 100	Bourns	CR0603-FX-1000ELF	Mouser	$0.05	1	$0.05
Resistor, 10k	Bourns	CR0603-JW-103ELF	Mouser	$0.10	2	$0.20
Resistor, 10m	Susumu	PRL0816-R010-F-T1	Mouser	$0.10	1	$0.10
Resistor, 150	Bourns	CR0603-FX-1500ELF	Mouser	$0.05	1	$0.05
Resistor, 18.2k	Bourns	CR0603-FX-1872ELF	Mouser	$0.05	1	$0.05
Resistor, 200	Bourns	CR0603-FX-2000ELF	Mouser	$0.05	1	$0.05
Resistor, 50	Vishay/Dale	CRCW060350R0FKEA	Mouser	$0.05	1	$0.05
Resistor, 6.19k	Bourns	CR0603-FX-6191ELF	Mouser	$0.05	1	$0.05
RF Antenna	Fastron	4408AF-103J-04	Mouser	$1.35	1	$1.35
RF Wakeup	ams	AS3930-BQFT	Mouser	$4.58	1	$4.58
SD-To-USB Converter	Maxim Integrated	MAX14502AETL+	Mouser	$22.35	1	$22.35
Battery 3.7V	-	-	Powerizer	$10.99	1	$10.99
Xbee	Digi International	-	Sparkfun	20.95	2	$41.90
RF 125kHz Signal Generator		ID-12	Sparkfun	$24.95	1	$24.95
PCB	-	-	-	$350.00	1	$350.00
					Total	$392.62